NASA/CR-2001-210648
ICASE Report No. 2001-1

Aerodynamic Shape Optimization of Two-dimensional Airfoils Under Uncertain Conditions

Luc Huyse
ICASE, Hampton, Virginia

R. Michael Lewis
The College of William & Mary, Williamsburg, Virginia

ICASE
NASA Langley Research Center
Hampton, Virginia

Operated by Universities Space Research Association

National Aeronautics and
Space Administration

Langley Research Center
Hampton, Virginia 23681-2199

Prepared for Langley Research Center
under Contract NAS1-97046

January 2001

AERODYNAMIC SHAPE OPTIMIZATION OF TWO-DIMENSIONAL AIRFOILS UNDER UNCERTAIN OPERATING CONDITIONS

LUC HUYSE* AND R. MICHAEL LEWIS†

Abstract. Practical experience with airfoil optimization techniques has revealed unexpected difficulties. Traditionally the performance of an airfoil is optimized for given, or assumed, model parameters. Experience has indicated that a deterministic optimization for discrete operating conditions may result in dramatically inferior performance when the actual conditions are different from these, somewhat arbitrarily chosen, design values. Extensions to multi-point optimization have proven unable to adequately remedy the problem of "localized optimization". This paper presents an intrinsically statistical approach and demonstrates how the shortcomings of multi-point optimization with respect to "localized optimization" can be overcome.

Key words. airfoil shape optimization, sensitivity analysis, statistical decision making, robust design, stochastic optimization, multi-point optimization

Subject classification. Applied and Numerical Mathematics

1. Introduction. Optimization of an analytical model is a process to develop better designs. Recent advances in computing power and the development of more accurate computational fluid dynamics codes (CFD) should, at least in theory, allow to compute the optimal shape of an airfoil for a particular application, specified by constraints on payload, range, etc. Unfortunately, practical experience suggests this is not the case. The use of deterministic optimization techniques leads to unexpected problems and often unacceptable results.

An important concern in the shape optimization of airfoils is the sensitivity of the final optimal design to small manufacturing errors or fluctuations in the operating conditions. Tightening the tolerances in the manufacturing process may prove prohibitively expensive or practically impossible to achieve. Moreover, a certain variability in the operating conditions (e.g. flight speed) cannot be avoided. Developing optimization methods which result in more "robust" designs sounds more appealing.

Several different approaches (Taguchi methods, bounds-based, minimax, fuzzy and probabilistic methods) can be taken to achieve "robustness" and a detailed review thereof is given in [7]. In this work we focus on Stochastic Optimization which tries to achieve the best performance (or minimal cost) for all possible combinations of the operating conditions. The paper focuses on the effectiveness of the optimization strategy rather than on particular implementations of optimization algorithms.

To our knowledge, non-deterministic approaches are quite new in aerodynamic optimization. In the next section an overview of existing deterministic attempts at introducing robustness is presented. Subsequently, we introduce an inherently statistical approach based on Van Morgenstern's Maximum Expected Value Criterion [9] and we conclude with an application.

*ICASE, Mail Stop 132C, NASA Langley Research Center, Hampton, VA 23681-2199 (email: l.huyse@larc.nasa.gov). This research was supported by the National Aeronautics and Space Administration under NASA Contract No. NAS1-97046 while the author was in residence at ICASE, NASA Langley Research Center, Hampton, VA 23681-2199.

†The College of William & Mary, P.O. Box 8795, 114 Jones Hall, Williamsburg, VA 23187-8795 (email: buckaroo@math.wm.edu). This research was supported by the National Aeronautics and Space Administration under NASA Contract No. NAS1-97046 while the author was in residence at ICASE, NASA Langley Research Center, Hampton, VA 23681-2199.

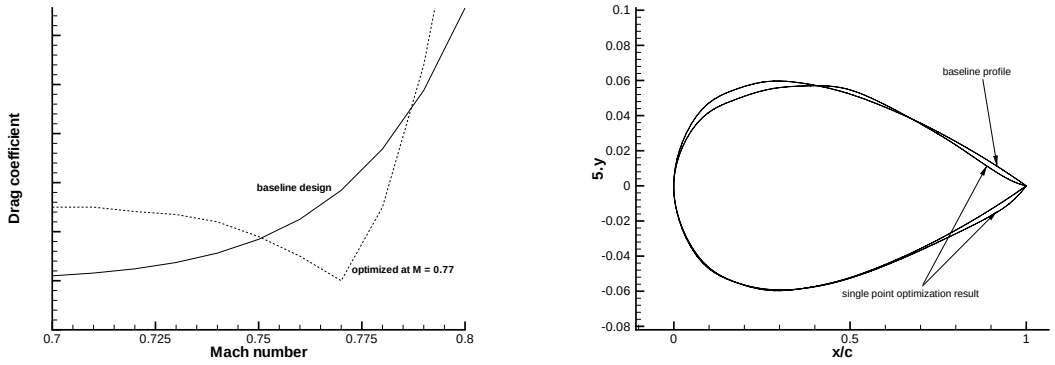

FIG. 2.1. *Single point optimization: (a) drag profile and (b) geometry*

2. Deterministic Approach to Airfoil Shape Optimization.

2.1. Formulation of Optimization Problem. In a deterministic context, aerodynamic shape optimization of airfoils is concerned with obtaining the most aerodynamically favorable geometry for fixed – either known or assumed – design conditions. In this approach, the requirements imposed on the design by other disciplines, such as sufficient strength and stiffness, are satisfied by introducing (in)equality constraints on some of the design variables. Mathematically, the objective function g, which depends on the design variables $\mathbf{d}$ and the model parameters θ is minimized over all possible designs, subject to n constraints:

$$\begin{cases} min_{\mathbf{d}\in\mathbf{D}}\ g(\mathbf{d},\theta) \\ subject\ to\ h_i(\mathbf{d},\theta) \geq 0 \quad for\ i = 1,...,n \end{cases} \tag{2.1}$$

This model is not necessarily an accurate reflection of the reality. The formulation in Eq.(2.1) contains no information regarding off-design condition performance. This is particularly worrisome if substantial variability is associated with any model parameter θ.

2.2. Single-Point Optimization. Consider the practical case where the drag C_d is to be minimized over a range of free flow Mach numbers M_∞:

$$\begin{cases} min_{\mathbf{d}\in\mathbf{D}}\ C_d(\mathbf{d},M_\infty) \\ subject\ to\ h_i(\mathbf{d},M_\infty) \geq 0 \quad for\ i = 1,...,n \end{cases} \tag{2.2}$$

Typically, constraints will be imposed on both the lift C_l and the geometry (minimum thickness of airfoil for sufficient strength)in Eq.(2.2). It is documented by other researchers [5] that, with this formulation, the drag reduction is attained only over a very narrow range (see Figure 2.1a). In the remainder of this paper, we will refer to this phenomenon as "localized optimization". Drela explains that the optimizer raises a "bump" on the airfoil to fill the transitional separation bubble (see Figure 2.1b). This effectively reduces the drag penalty which occurs when a bubble undergoes transition and reattachment [4]. However, the location of this bubble varies with M_∞ and this explains the really poor behavior in off-design conditions.

It can be concluded that the real problem is not with the optimizer, which is likely to perform just fine, but with the problem formulation of Eq.(2.2). Trade-offs between different design conditions should explicitly be considered in the problem formulation.

2.3. Multi-Point Optimization. A straightforward approach to consider different M_∞ is to generalize the objective in Eq.(2.1) to a linear combination of flight conditions (m in total):

$$\begin{cases} min_{\mathbf{d}\in\mathbf{D}} \sum_i^m w_i C_d(\mathbf{d}, M_{\infty,i}) \\ subject\ to\ h_j(\mathbf{d}, M_{\infty,i}) \geq 0 \qquad for\ j = 1, ..., n \end{cases} \tag{2.3}$$

Practical problems arise with the selection of the flight conditions $M_{\infty,i}$ and with the specification of the weights. There is no clear theoretical principles to guide the selection, which is in fact largely left up to the designer's discretion (see [3], [5], [6]).

With the multi-point formulation, an improved C_d can be realized over a wider range of Mach numbers M_∞ [5]. However, this formulation is still unable to provide a truly global solution by avoiding localized optimization. In fact multiple "bumps" appear on the airfoil, one associated with each flight condition $M_{\infty,i}$. In the transonic regime, each bump occurs at the shock foot location for each of the sampled Mach numbers.

3. Explicitly Statistical Approach.

3.1. Design as a Decision-Making Process. Designing a structure or device is essentially a decision-making process. Appropriate values of the design variables $\mathbf{d}$ need to be selected which optimize the performance or the utility of a design. The designer has full control over the design variables, such as the geometry of the structure and the type and grade of materials used for it, but the operating conditions of a structure or device, such as the loads or the operating speeds, will typically vary during the design life time.

Since each operating condition parameter may take on a range of values over the lifetime of the design, it is possible to collect their histograms (and joint histograms). From a subjectivist point of view, the operating conditions are then effectively modeled as random variables.

The previous section indicated that a specific design may perform exceptionally well for a selected set of operating conditions, say the free flow Mach number M_∞, but may perform poorly for slightly different values of M_∞, which are quite likely to occur. The impact of the uncertainty of M_∞ on the design performance should be taken into account when the quality of a particular design is assessed.

3.2. Mathematical Problem Formulation. To avoid overloading the notation, we will resort to our basic problem in Eq.(2.2): minimize the drag C_d over a range of free flow Mach numbers M_∞ while maintaining lift $C_l = C_l^*$. Note that M_∞ is now a random variable. The optimization problem Eq.(2.2) is now interpreted as a statistical decision-making problem.

According to the Von Neumann-Morgenstern statistical decision theory [9], the best course of action in the presence of uncertainty is to select the design which leads to the lowest expected drag. This is commonly known as the Maximum Expected Value criterion (MEV). The risk ρ, associated with a particular design $\mathbf{d}$, is identified as the expected value of the perceived loss associated with the design. The best design or decision, which minimizes the overall risk, is referred to as the "Bayes' decision". In our problem formulation, the Bayes' risk ρ^* and Bayes' decision $\mathbf{d}^*$ are given as:

$$\begin{cases} \rho^* & = \int_{M_\infty} C_d(\mathbf{d}^*, M_\infty) f_{M_\infty}(M_\infty) dM_\infty \\ & = min_{\mathbf{d}\in D} \int_{M_\infty} C_d(\mathbf{d}, M_\infty) f_{M_\infty}(M_\infty) dM_\infty \\ subject\ to\ C_l(\mathbf{d}, M_\infty) = C_l^* \end{cases} \tag{3.1}$$

where $f_{M_\infty}(M_\infty)$ is the probability density function of M_∞.

The practical problem with formulation Eq.(3.1) is that integration is required in each of the optimization steps. Since the objective function C_d is computationally expensive to evaluate, this approach, although theoretically sound, becomes prohibitively expensive. Therefore a computational scheme that minimizes the number of function calls is desirable.

3.3. Analytic Approximation of the Expectation Integral. When the variability of the free flow Mach number M_∞ is not too large, a second-order Taylor series expansion of C_d around the mean value $\overline{M}_\infty$ may be a sufficiently accurate model of the variation of the drag C_d with respect to M_∞.

$$C_d(\mathbf{d}, M_\infty) \simeq C_d(\mathbf{d}, \overline{M}_\infty) + \nabla_{M_\infty} C_d.(M_\infty - \overline{M}_\infty) + \tfrac{1}{2}\nabla^2_{M_\infty} C_d.(M_\infty - \overline{M}_\infty)^2 \tag{3.2}$$

When substituted in the Bayes' risk expression (3.1), the linear term $\nabla_{M_\infty} C_d.(M_\infty - \overline{M}_\infty)$ in Eq.(3.2) disappears after integration over M_∞ because the Taylor series is built around the mean value $\overline{M}_\infty$. The Bayes' risk is:

$$\begin{cases} \rho^* = min_{\mathbf{d}\in D}\left[C_d(\mathbf{d}, M_\infty) + \frac{1}{2}Var(M_\infty)\left.\frac{\partial^2 C_d}{\partial {M_\infty}^2}\right|_{\mathbf{d},\overline{M}_\infty}\right] \\ subject\ to\ C_l(\mathbf{d}, M_\infty) = C_l^* \end{cases} \tag{3.3}$$

It seems that we have substituted an integration with an almost equally expensive computation of a second-order derivative. Even though the approximation may result in only moderate computational savings, this theoretical result provides additional insight in the problem. It follows from Eq.(3.3) that the variability of M_∞ can affect the optimal design only if the objective function C_d is highly non-linear in this parameter. This is the case near the drag divergence Mach number M_{DIV}, where the drag undergoes a sharp increase.

In mathematical terms, the advantage of working with expected values is that the minimum is second-order accurate with respect to variations in the parameters. This ensures a more global solution since localized optimization will be avoided. This can also be explained in an intuitive manner: the second-order derivative is a measure for the curvature. Since this curvature is now a part of the objective function, a design which results in a drag trough or "cusp" as found in the optimal solution in Figure 2.1a will not be accepted by the optimizer. The high curvature of the "cusp" would increase the objective in Eq.(3.3) and excessive localized optimization will be avoided.

3.4. Direct Numerical Evaluation of Expectation and Comparison with Multi-Point Optimization. The integration with respect to M_∞ in Eq.(3.1) can also be performed numerically. Irrespective of the chosen integration scheme, the optimization problem (3.1) can formally be rewritten as (n_k integration points):

$$\rho = min_{\mathbf{d}\in D}\left(\sum_{k=1}^{n_k} w_k.C_d(\mathbf{d}, M_{\infty,k}) + \epsilon(n_k)\right) \tag{3.4}$$

where the integration error $\epsilon(n_k) \to 0$ as $n_k \to \infty$.

Formulation Eq.(3.4) is strikingly similar to Eq.(2.3). It is therefore interesting to analyze how the Bayes' decision $\mathbf{d}^*$ – which minimizes ρ in Eq.(3.4)– compares with the multi-point solution and exactly how localized optimization is avoided.

In the multi-point approach the Mach numbers and weights need to be selected by the designer. In the statistical approach, the weights are directly related to the relative importance of each Mach number

through the integration over the probability density. Which Mach numbers are used in the optimization depends on the chosen integration scheme. In short, the statistical approach removes the arbitrariness from the weighting process.

Careful comparison of Eq.(2.3) with Eq.(3.4) reveals the shortcoming in the multi-point formulation which causes localized optimization. Numerical integration of Eq.(3.1) results in Eq.(3.4) and includes a random, zero-mean error term $\epsilon(n_k)$, which decreases as the number of sampling points increases. The multi-point optimization Eq.(2.3) differs from Eq.(3.4) only in the sense that this error term is not explicitly considered in the objective function. However, omitting this error term from the optimization problem alters the structure of the problem at hand. The multi-point optimization effectively looks for the design, which minimizes the weighted sum of the goal function C_d, evaluated in the n_k specified points $M_{\infty,k}$. There is absolutely no control over what happens to the objective function C_d in the neighborhood around these n_k sampling points. During the optimization iterations, the shape of the goal function $C_d(\mathbf{d}, M_\infty)$ is altered. As a result, the discrete sum in Eq.(2.3) may fail to be a good approximation of the integral in Eq.(3.1).

In effect, multi-point optimization will prefer a design $\mathbf{d}_1$ over a design $\mathbf{d}_2$ even when design $\mathbf{d}_1$ is considerably worse than design $\mathbf{d}_2$ in all but the n_k specified sampling points. Multi-point optimization allows the optimizer to mold the goal function C_d to its own advantage. What was originally a random integration error is no longer random, and the discrete sum in Eq.(2.3) no longer approximates the integral in Eq.(3.1) at all.

This rather annoying behavior is avoided if we can prevent the optimizer from exploiting the approximation error in Eq.(3.4) to its own advantage. We need to make sure that the discrete sum in Eq.(3.4) really is an approximation of the integral in Eq.(3.1) at all times. In general terms, we need to ensure that the discrete sum Eq.(2.3) remains a a good approximation of the integral in Eq.(3.1). An elegant solution is to randomize the sampling points $M_{\infty,k}$ in the evaluation of the integral but any adaptive optimization scheme that varies the location of the integration points $M_{\infty,k}$ for each optimization step will do. Randomization of the integration points ensures that the optimizer maximizes the performance not just for n_k specific values of $M_{\infty,k}$, but for any set of values $M_{\infty,k}, k = 1, \ldots n_k$. To minimize the loss of accuracy in the integration due to random location of the integration points, stratified sampling can be used to generate the $M_{\infty,k}$ values. Our experience with the spline-based integration also suggests that the sampling points should not be allowed to be arbitrarily close to each other.

3.5. Additional Considerations. The use of Eq.(3.4) for the optimization instead of Eq.(2.3) leads to numerical complications. Because of the random location of the integration points $M_{\infty,k}$, a repeated evaluation of the objective function C_d for identical values of the design parameters $\mathbf{d}$ will lead to different results. This makes it hard to identify whether a new design is really better than a previous one, or if the "improvement" should be attributed to random fluctuations instead. When a trial solution $\mathbf{d}$ is still far away from the optimal solution $\mathbf{d}^*$, large improvements ΔC_d can be expected. This means that a very crude integration, which requires very few function evaluations, will suffice in the early stages of the optimization. The improvement of the goal function is expected to be smaller closer to the optimal solution, and more sampling points $M_{\infty,k}$ will be required to keep the integration error small enough. Current research focuses on the development of a strategy which takes maximum advantage of this effect.

In addition, the physical and mathematical models used for the objective function will generally not be error-free. Each of these errors can be treated as a random variable. Their effect on the optimal solution is readily assessed by extending the integration over these additional random variables. It is believed that the approximate second-order result in Eq.(3.3) will prove particularly useful for this purpose. In a first step we

minimize the drag while keeping the model errors fixed at their average level. If the second order derivative of the drag with respect to this model error parameter at the solution of this simplified problem (without explicit error modeling) is sufficiently small, it can be concluded that these model errors will only have a minimal impact on the solution. Otherwise, the model errors should explicitly be included in the problem formulation and a full integration is required.

4. Application: 2D-Airfoil in Transonic Regime.

4.1. Problem Formulation. In this section the presented method is applied to a practical transonic optimization problem: lift-constrained ($C_l^* = 0.175$) minimization of the drag C_d for a Mach number range $M_\infty \in [0.7, 0.8]$ (we assumed a uniform distribution for M_∞). In this analysis only the Mach number is considered an uncertain operating variable; no additional model uncertainties are included. No constraints are imposed on the pitching moment C_m. The baseline geometry is a NACA-0012 profile, which was splined using 23 control nodes. The design variables in the optimization problem are given by the vertical positions of the control nodes and the angle of attack α. Three control nodes are in locked positions: one at the leading edge, and a double control node at the trailing edge. The inviscid Euler equations for the flow are discretized on unstructured meshes [2]. The sensitivities of both lift and drag with respect to the design parameters are efficiently calculated using a continuous adjoint formulation [1]. We used a bound constrained trust region algorithm in the optimization [8]. The following optimization formulations are compared:

1. optimization at the midpoint of the Mach range: $M_\infty = 0.75$
2. multipoint optimization using 4 Mach numbers: $M_\infty = 0.72, 0.74, 0.76$ and 0.78
3. "robust" optimization using 4 randomly selected Mach numbers

In formulations 2 and 3, the integration is performed using interpolating natural splines, which are based on 5^{th}-order Hermite-polynomials. Formulations 2 and 3 require a similar amount of computational effort.

4.2. Single-Point Optimization Results. The single point case has 21 design variables: the angle of attack α and the vertical positions of the 10 spline control nodes at both the top and bottom surface of the airfoil. Table 1 indicates a dramatic reduction of the drag C_d is obtained at $M_\infty = 0.75$, but Figure 2.1a reveals that this gain is rapidly lost when the free flow Mach number is away from this design value.

The geometry plot in Figure 2.1b shows what happens. During the optimization a distinct "bump" is formed on the top surface. The optimizer takes advantage of all degrees of freedom to achieve the lowest possible drag at $M_\infty = 0.75$, irrespective of what happens to the drag at other Mach numbers. Obviously, there is a penalty to be paid for this: even though the drag reduction at the design Mach number is 24%, the reduction over the entire Mach range is only 11% (see Table 1). This localized optimization behavior was previously documented by Drela [5].

4.3. Multi-Point Optimizations. The constrained multi-point optimization has 24 design variables: the same 20 y-coordinates which describe the geometry and 4 angles of attack. The optimal angle of attack (which ensures that the lift constraint is satisfied)depends on the free flow Mach number, so each design condition adds one additional angle-of-attack design variable. The integration of the drag over the Mach range is performed using spline-based inter/extrapolation for both the fixed point and robust optimizations.

The results in Table 1 indicate that a multi-point optimization does indeed achieve a better overall drag reduction: the discrepancy between the drag reduction at the design points (18%) and the true drag reduction over the entire range (15.5%) is significantly reduced. This is in line with the findings of other researchers [5]. However, Figure 4.1 indicates a drag-trough at or near each of the discrete design points.

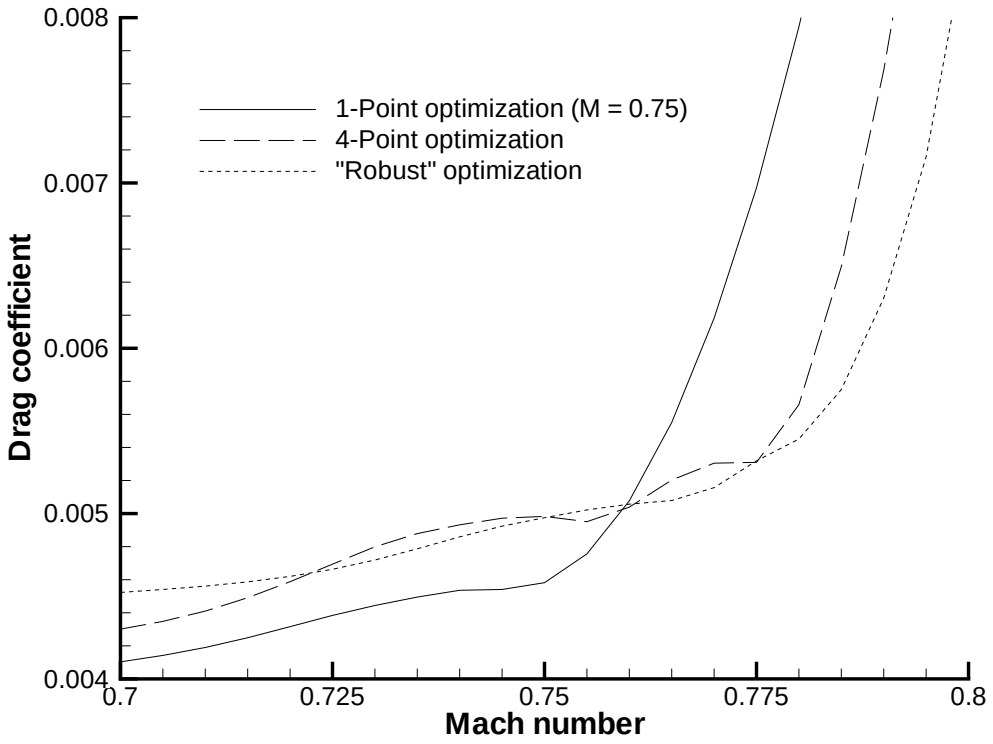

FIG. 4.1. *Drag profile obtained using different optimization strategies*

TABLE 4.1
Comparison of drag improvements for different optimization formulations

Optimization Model	Reduction at Sampling Points	Reduction of Expected Value
Single Point	24%	11%
4-Point Fixed	18%	15.5%
4-Point Robust	N/A	17.5%

The drag increases rapidly away from the design points. This is very clear near the high end of the Mach range.

Figure 4.1 shows that the "robust" optimization scheme with randomly selected values for M_∞ results in a much smoother drag profile over the entire Mach range. The resulting airfoil geometry is a lot smoother as well. In this particular case the drag reduction over the entire interval is 17.5%, almost identical to the drag reduction at the design points for the multipoint optimization with 4 points. It can be concluded that the "robust" scheme results in a superior design for an identical computational effort. It is interesting to note that the final geometries are quite different for each method: one solution requires a much higher angle of attack than the other.

5. Summary and Conclusions. The robustness of an optimal solution can be achieved by incorporating the variability of the operating conditions directly into the optimization problem formulation. The

practical application shows that a statistical approach leads to smooth airfoil geometries and drag profiles.

The suggested method is computationally similar to existing multi-point optimization, which is widely accepted in industry. This increases the likelihood of acceptance by both designers and theorists alike. The new formulation avoids the arbitrary selection of design conditions and weighting factors; they automatically follow from the procedure.

The relative likelihood of each operating condition is taken into account. A randomized integration scheme ensures that the optimizer cannot exploit approximation errors due to discretization.

It can be concluded that optimization on the basis of the Euler equations leads to some interesting candidate designs. However, viscous effects need to be included to achieve more realistic pressure distributions.

6. Acknowledgments. The authors are indebted to Sharon L. Padula of the NASA Langley Research Center's Multidisciplinary Optimization Branch and William A. Crossley of the Purdue University School of Aeronautics and Astronautics for their insightful comments and suggestions.

REFERENCES

[1] W.K. Anderson and V. Venkatakrishnan, *Aerodynamic Design Optimization on Unstructured Grids with a Continuous Adjoint Formulation*, AIAA-97-0643, 1997.

[2] W.K. Anderson and D.L. Bonhaus, *Aerodynamic Design on Unstructured Grids for Turbulent Flows*, NASA TM-112867, NASA Langley Research Center, VA, 1997.

[3] R.L. Campbell, *Efficient Viscous Design of Realistic Aircraft Configurations*, AIAA-98-2539, 1998.

[4] M. Drela, *Low Reynolds number airfoil design for the MIT Daedalus prototype: A case study*, Journal of Aircraft, 25, No. 8 (1988), pp. 724-732.

[5] M. Drela, *Pros & Cons of Airfoil Optimization*, MIT, personal communication, 1998.

[6] J. Elliott and J. Peraire, *Constrained, Multipoint Shape Optimization for Complex 3D Configurations*, Aeronautical Journal, 102, No. 1017 (1998), pp. 365-376.

[7] L. Huyse, *Solving Problems of Optimization Under Uncertainty as Statistical Decision Problems*, AIAA-2001-1519, 2001.

[8] L. Kaufman and D. Gay, *PORT Library: Optimization and Mathematical Programming*, Bell Laboratories, 1997.

[9] J.W. Pratt, H. Raiffa and R. Schlaifer, *Introduction to Statistical Decision Theory*, Cambridge: MIT Press, 1986.